Journal of the Serbian Society for Computational Mechanics / Vol. 17 / No. 2, 2023 / pp 142-152
(10.24874/jsscm.2023.17.02.10)

FINITE ELEMENT SIMULATION FOR THE PLASTIC BEHAVIOR OF CORRUGATED CORE SANDWICH PANEL

Dao Lien Tien[1], Nguyen Thi Thu Phuong[2], Duong Pham Tuong Minh[1] and Viet Dung Luong[1*]

[1] Faculty of Mechanical Engineering, Thai Nguyen University of Technology, Vietnam
e-mail: daotien@tnut.edu.vn, tuongminh80@tnut.edu.vn, luongvietdung@tnut.edu.vn
[2] Faculty of Engineering Technology, Hung Vuong University, Vietnam
e-mail: nguyenthuphuong@hvu.edu.vn
**corresponding author*

Abstract

Nowadays, numerical simulation methods have been widely applied in product design and development, especially in sandwich panel design. However, such numerical models need to be built to optimize calculation time. In this paper, we propose a finite element model to study the plastic mechanical behavior of corrugated sandwich panels. Accordingly, a 2D finite element equivalent model is built by the homogenization method to replace the 3D model. This model greatly reduces the computation time as well as the model building time. The accuracy of the proposed model is confirmed by comparing the numerical simulation results of the 2D equivalent model with the 3D model and experimental results.

Keywords: Homogenization, Finite element, Simulation, Corrugated, Bending test.

1. Introduction

Today, the industry is facing the challenge of reducing the volume of parts, and structures. One of the solutions is to use a corrugated and honeycomb panel structure. These structures have high stiffness and a high strength-to-weight ratio of the sandwich panels. The sandwich panel structure consists of a lightweight core and rigid outer layers. The core may consist of a continuous or discrete structural component. Core shapes are diverse such as corrugation, honeycomb, foam, triangle, etc. Among them, corrugated cardboard is one of the widely used structures in the packaging industry. It is made up of layers of paper, corrugated, usually at least two layers of paper and one layer of corrugated board. The manufacturing process gives three characteristic directions: the machine direction (MD), the cross direction (CD), and the thickness direction (ZD) (Fig. 1).

Up to now, there have been many studies on sandwich panel structures. Z. Aboura et al. (2004) have proposed a model to study the elastic behavior of corrugated cardboard. The model shows that the E_{MD} modulus and bending properties (D11 and D22) are strongly influenced by the total sheet thickness while the E_{CD} modulus is more influenced by the grooving step and other studies such as those of Wan-Shu Chang and T. Krauthammer (2006), Kyung-Jo Park et al. (2016), Cenk Kılıçaslan et al. (2013), M.R.M. Rejab et al. (2013), Xiaoxia Huang et al. (2020).

Besides, with the development of science and technology, design calculation has been supported by computers. However, calculating these structures takes a long time, and often requires a high-configuration computer. By using the finite element method, the mechanical behavior of the panels is determined, but with the complex 3D modeling of the corrugated board, numerical modeling and simulation will be time-consuming and may not be possible with large panels. The homogenization method is used to simplify the simulation process, the corrugated board will be replaced by an equivalent solid 3D or 2D sheet. N. Talbi et al. (2009) also developed a homogeneous analysis model based on multilayer laminate theory and compared its results with numerical and experimental results. Biancolini et al. (2017) used the finite element analysis (FEA) to evaluate the stiffness parameters, Rajesh Kumar Boorle (2014), and Marc R. Schultz et al. (2011) presented the homogenous properties such as cross-sectional stiffness and flexural stiffness of corrugated board by analytical method. T.J. Lu et al. (2005), PTM Duong et al. (2012), and Jongmin Park et al. (2020) have demonstrated some of the properties of the corrugated board by analytical methods. Damian Mrówczyński and Tomasz Garbowski (2023) proposed a finite element model based on the equivalence of strain energy between the 3D model and the simplified model to study the behavior of five-layered cardboard. In another study, using finite element modeling, Damian Mrówczyński et al. (2022) found a general geometry that reflects possible imperfections to accurately determine the effective parameters of a periodic core for a homogeneous plate. However, most of these studies are limited to the behavior of sandwich panels in the elastic region.

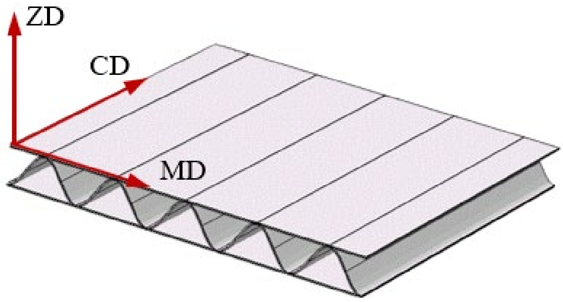

Fig. 1. The directions of the corrugated cardboard plate.

Besides, in published studies related to numerical simulation for this type of structure, almost no research has mentioned the calculation time and geometric modeling time of this structure. Using full 3D models for sandwich structures is time-consuming. To reduce model preparation and computational time, we have developed a plastic homogenization model for corrugated cardboard based on established homogenization modeling techniques. The model is then imported into the Abaqus software with the help of a subroutine to perform numerical simulations for the plate in tension and bending. The accuracy of this equivalent model is confirmed by comparing the results obtained with those of 3D structural panels and experimental results.

2. Homogenization model

The homogenization method is based on Mindlin's theory and the multi-layer plate theory for thick or composite plates. It assumes that a segment that is straight and perpendicular to the mean surface remains straight but not perpendicular to the mean surface after the deformation. This assumption makes it possible to consider the deformations of transverse shearing. On the mean surface of a plate, we define the x and y-axes on the surface and the z-axis perpendicular to the surface (Fig. 2,3,4), Mindlin's theory assumes the following displacement field.

$$\begin{cases} u_q = u + z\beta_x \\ v_q = v + z\beta_y \\ \mathrm{w}_q = \mathrm{w} \end{cases} \tag{1}$$

where u_q, v_q, and w_q are the displacements of a point $q(x, y, z)$, u, v and w are the displacements of the point $p(x, y, 0)$ on the mean surface, β_x is the angle of rotation of the normal from z to x or the angle of rotation around y ($\beta_x=\theta_y$), βy is the angle of rotation from the normal from z to y or the angle of rotation around $-x$ ($\beta_y = -\theta_x$).

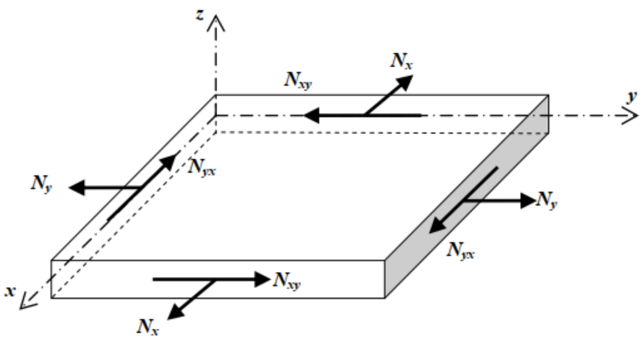

Fig. 2. Membrane forces on a plate.

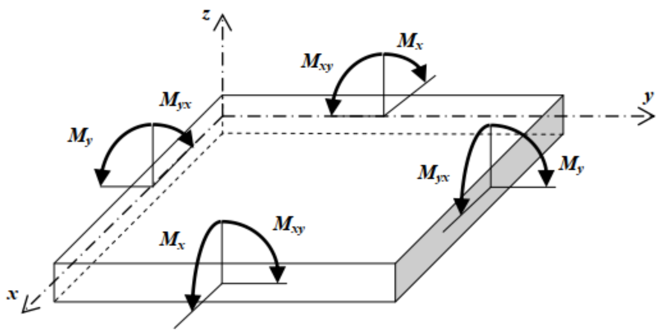

Fig. 3. Bending-torsional moments on a plate.

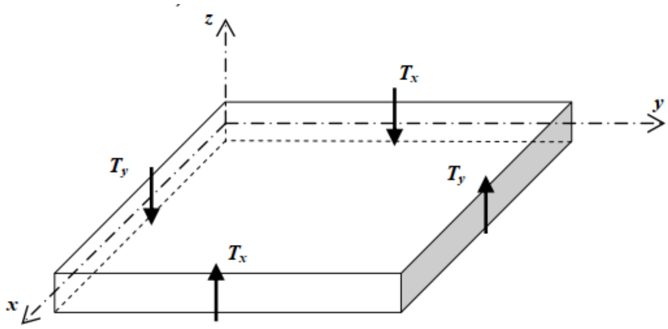

Fig. 4. Transverse shear forces on a plate.

The deformation field is written as follows:

$$\begin{cases} \varepsilon_x = u_q,_x = u,_x + z\beta_x,_x \\ \varepsilon_y = v_q,_y = v,_y + z\beta_y,_y \\ \gamma_{xy} = 2\varepsilon_{xy} = u_q,_y + v_q,_x = u,_y + v,_x + z(\beta_x,_y + \beta_y,_x) \\ \gamma_{xz} = 2\varepsilon_{xz} = u_q,_z + w_q,_x = w,_x + \beta_x \\ \gamma_{yz} = 2\varepsilon_{yz} = v_q,_z + w_q,_y = w,_y + \beta_y \\ \varepsilon_z = w_q,_z = 0 \end{cases} \tag{2}$$

Plane strains can be decomposed into the membrane and bending strains as follows:

$$\{\varepsilon\} = \{\varepsilon_m\} + z\{\kappa\} \tag{3}$$

$$\{\sigma\} = \begin{Bmatrix} \sigma_x \\ \sigma_y \\ \sigma_{xy} \end{Bmatrix} = [Q]\begin{Bmatrix} \varepsilon_x \\ \varepsilon_y \\ \gamma_{xy} \end{Bmatrix} = \begin{bmatrix} \frac{E_x}{1-\nu_{xy}\nu_{yx}} & \frac{\nu_{xy}E_y}{1-\nu_{xy}\nu_{yx}} & 0 \\ \frac{\nu_{yx}E_x}{1-\nu_{xy}\nu_{yx}} & \frac{E_y}{1-\nu_{xy}\nu_{yx}} & 0 \\ 0 & 0 & G_{xy} \end{bmatrix} \begin{Bmatrix} \varepsilon_x \\ \varepsilon_y \\ \gamma_{xy} \end{Bmatrix} \tag{4}$$

$$\{\sigma_\gamma\} = \begin{Bmatrix} \sigma_{xz} \\ \sigma_{yz} \end{Bmatrix} = [C]\begin{Bmatrix} \gamma_{xz} \\ \gamma_{yz} \end{Bmatrix} = \begin{bmatrix} G_{xz} & 0 \\ 0 & G_{yz} \end{bmatrix} \begin{Bmatrix} \gamma_{xz} \\ \gamma_{yz} \end{Bmatrix} \tag{5}$$

The membrane forces, the bending, and torsion moments:

$$\{N(x,y)\} = \begin{bmatrix} N_x \\ N_y \\ N_{xy} \end{bmatrix} = \int_{-\frac{h}{2}}^{\frac{h}{2}} \begin{bmatrix} \sigma_x \\ \sigma_y \\ \sigma_{xy} \end{bmatrix} dz \tag{6}$$

$$\{M(x,y)\} = \begin{bmatrix} M_x \\ M_y \\ M_{xy} \end{bmatrix} = \int_{-\frac{h}{2}}^{\frac{h}{2}} z \begin{bmatrix} \sigma_x \\ \sigma_y \\ \sigma_{xy} \end{bmatrix} dz \tag{7}$$

$$\{T(x,y)\} = \begin{bmatrix} T_x \\ T_y \end{bmatrix} = \int_{-\frac{h}{2}}^{\frac{h}{2}} \begin{bmatrix} \sigma_{xz} \\ \sigma_{yz} \end{bmatrix} dz \tag{8}$$

After the integration according to the thickness, one obtains the matrix of the total rigidities which binds the generalized deformations to the resulting efforts:

$$\begin{Bmatrix} N_x \\ N_y \\ N_{xy} \\ M_x \\ M_y \\ M_{xy} \\ T_x \\ T_y \end{Bmatrix} = \begin{bmatrix} A_{11} & A_{12} & 0 & B_{11} & B_{12} & 0 & 0 & 0 \\ A_{12} & A_{22} & 0 & B_{12} & B_{22} & 0 & 0 & 0 \\ 0 & 0 & A_{33} & 0 & 0 & B_{33} & 0 & 0 \\ B_{11} & B_{12} & 0 & D_{11} & D_{12} & 0 & 0 & 0 \\ B_{12} & B_{22} & 0 & D_{12} & D_{22} & 0 & 0 & 0 \\ 0 & 0 & B_{11} & 0 & 0 & D_{33} & 0 & 0 \\ 0 & 0 & 0 & 0 & 0 & 0 & F_{11} & 0 \\ 0 & 0 & 0 & 0 & 0 & 0 & 0 & F_{22} \end{bmatrix} \begin{Bmatrix} \varepsilon_x \\ \varepsilon_y \\ \gamma_{xy} \\ \kappa_x \\ \kappa_y \\ \kappa_{xy} \\ \gamma_{xz} \\ \gamma \end{Bmatrix} \tag{9}$$

$$A_{ij} = \sum_{k=1}^{n} \left[h^k - h^{k-1} \right] Q_{ij}^k = \sum_{k=1}^{n} Q_{ij}^k t^k \tag{10}$$

$$B_{ij} = \frac{1}{2} \sum_{k=1}^{n} \left[\left(h^k\right)^2 - \left(h^{k-1}\right)^2 \right] Q_{ij}^k = \sum_{k=1}^{n} Q_{ij}^k t^k z^k \tag{11}$$

$$D_{ij} = \frac{1}{3} \sum_{k=1}^{n} \left[\left(h^k\right)^3 - \left(h^{k-1}\right)^3 \right] Q_{ij}^k = \sum_{k=1}^{n} Q_{ij}^k \left[t^k \left(z^k\right)^2 + \frac{\left(t^k\right)^3}{12} \right] \tag{12}$$

$$F_{ij} = \sum_{k=1}^{n} \left[h^k - h^{k-1} \right] C_{ij}^k = \sum_{k=1}^{n} C_{ij}^k t^k \tag{13}$$

where A_{ij} represents the stiffness of the membrane, D_{ij} represents the stiffness of bending and torsion, F_{ij} represents the stiffness of transverse shears and B_{ij} represents the terms of coupling between membrane and bending-torsion. If the composite plate is symmetric with respect to its average surface, this coupling disappears, and B_{ij}=0.

Homogenization consists of representing a sandwich panel by a homogeneous plate using the periodic unit cell of corrugated cardboard represented in Fig. 5, where the local reference of the groove is defined using the angle $\theta_{(x)}$:

$$\begin{cases} \theta(x) = \tan^{-1}\left(\dfrac{dh(x)}{dx} \right) \\ h(x) = \left(\dfrac{h_c}{2} - \dfrac{t_2}{2} \right) \sin\left(2\Pi \dfrac{x}{p} \right) \end{cases} \tag{14}$$

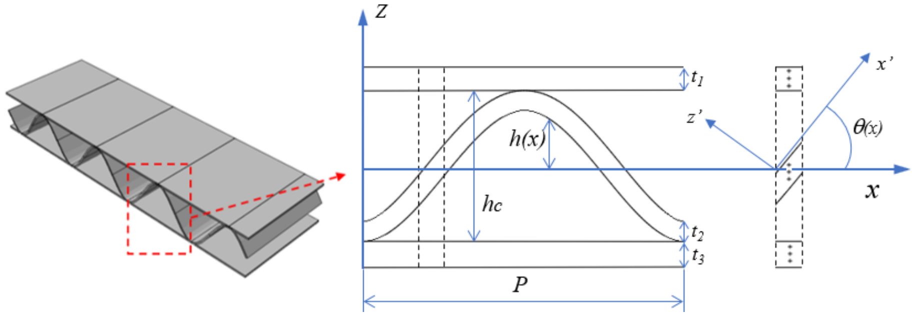

Fig. 5. Periodic unit cell of a corrugated cardboard and numerical integration points through the thickness.

The simplifying assumptions as well as the calculations of the different stiffnesses are given in the study of A V. Dung Luong et al (2018), Luong, V. D. et al. (2020). The plastic behavior of each stratum of the corrugated board (*skins and flutes*) can be represented by the isotropic plasticity equivalent (IPE) model in the study of Mäkelä P (2003). The orthotropic elasticity behavior in plane stresses is defined by:

$$\{\sigma\}=\begin{Bmatrix}\sigma_x\\ \sigma_y\\ \sigma_{xy}\end{Bmatrix}=[H]\{\varepsilon^e\}=\frac{1}{(1-\nu_{xy}\nu_{yx})}\begin{bmatrix}E_x & \nu_{yx}E_x & 0\\ \nu_{xy}E_y & E_y & 0\\ 0 & 0 & G_{xy}(1-\nu_{xy}\nu_{yx})\end{bmatrix}\begin{Bmatrix}\varepsilon_x^e\\ \varepsilon_y^e\\ \gamma_{xy}^e\end{Bmatrix} \tag{15}$$

The deviatoric stresses vector and the IPE plasticity criterion are given by:

$$\{s\}=\begin{Bmatrix}s_x\\ s_y\\ s_z\\ s_{xy}\end{Bmatrix}=[L]\{\sigma\}=\frac{1}{3}\begin{bmatrix}2A & C-A-B & 0\\ C-A-B & 2B & 0\\ B-C-A & A-B-C & 0\\ 0 & 0 & 3D\end{bmatrix}\begin{Bmatrix}\sigma_x\\ \sigma_y\\ \sigma_{xy}\end{Bmatrix} \tag{16}$$

$$f=\sigma_{eq}-Y=\left(\frac{3}{2}\langle s\rangle\{s\}\right)^{1/2}-E_0\left(\varepsilon_0+\varepsilon_{eq}^p\right)^{1/n}=0 \tag{17}$$

where Y is the yield stress, A, B, C, D, E_0, ε_0, ε_{eq}^p, n are the parameters of the IPE model that can be determined using experimental tests.

To determine the equivalent tangent matrix of the corrugated cardboard, we use three integration points according to the thickness of each of its layers. The plasticity algorithm developed for compact cardboard is used for each of the layers at each integration point to determine the stress state and the tangent matrix in the local coordinate system of each layer k: $\left[Q_p^{(k)}\right]$

Membrane forces, bending moments, and torsion are obtained by integrating the constraints against the sheet thickness by replacing the elastic matrices $[Q^{(k)}]$ with tangent matrices $[Q_p^{(k)}]$ in equations (10), (11), and (12) to arrive at terms of the overall stiffness matrix:

$$A_{ij}(x)=\frac{t_1}{2}\sum_{k=1}^{3}Q_{pij}^{(1)}w_k+\frac{t_2}{2\cos\theta(x)}\sum_{k=1}^{3}Q_{pij}^{(2)}\left(\theta(x)\right)w_k+\frac{t_3}{2}\sum_{k=1}^{3}Q_{pij}^{(3)}w_k \tag{18}$$

$$B_{ij}\left(x\right)=\frac{t_1}{2}\sum_{k=1}^{3}Q_{pij}^{(1)}z_k w_k+\frac{t_2}{2\cos\theta(x)}\sum_{k=1}^{3}Q_{pij}^{(2)}\left(\theta\left(x\right)\right)z_k w_k+\frac{t_3}{2}\sum_{k=1}^{3}Q_{pij}^{(3)}z_k w_k \tag{19}$$

$$D_{ij}\left(x\right)=\frac{t_1}{2}\sum_{k=1}^{3}Q_{pij}^{(1)}z_k^2 w_k+\frac{t_2}{2\cos\theta(x)}\sum_{k=1}^{3}Q_{pij}^{(2)}\left(\theta\left(x\right)\right)z_k^2 w_k+\frac{t_3}{2}\sum_{k=1}^{3}Q_{pij}^{(3)}z_k^2 w_k \tag{20}$$

where w_k represents the numerical integration weight corresponding to the point of integration k of the considered layer. The plastic homogenization model of corrugated cardboard has been implemented in the Abaqus/Standard computer code using the user subroutine UGENS.

3. Numerical validation of the equivalence model

3.1. Validation of the equivalence model by simulation of tensile test

We used corrugated cardboard material in this study with the properties shown in Fig. 6 and given in Table 1 and Table 2.

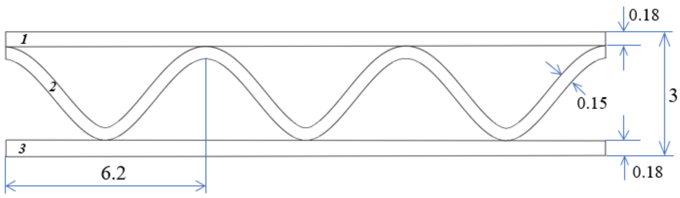

Fig. 6. Geometric structure of the corrugated cardboard plate.

Paper	E_x (MPa)	E_y (MPa)	ν_{xy}	G_{xy} (MPa)	E_0
1,3	2350.2	879.91	0.0829	1047.2	91.45
2	1120.4	615.85	0.0717	301.05	80.31

Table 1. Properties elastic of the papers.

Paper	n	A	B	C	D	ε_0
1,3	3.807	1.0	2.136	2.136	1.422	0.48e-3
2	3.047	1.0	2.718	2.136	1.571	0.92e-3

Table 2. Properties plastic of the papers.

Simulations of tensile tests in the MD, CD and 45° directions are carried out using the proposed homogenization model and the complete model. The dimensions of the specimen (for the two models are the same (Fig. 7). The 3D structure and the homogenized plate mesh with reduced integration rectangular shell elements (S4R) with a size of 0.4 mm.

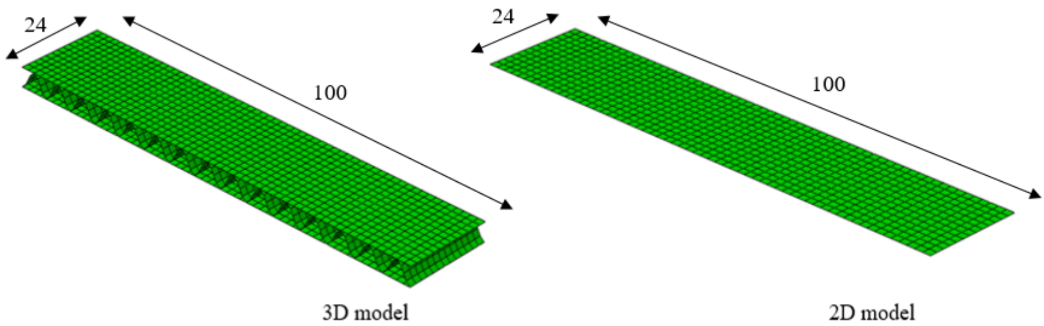

Fig. 7. Meshes of the corrugated cardboard 3D structure and the 2D homogenized plate.

Figure 8 shows the comparison of the force-elongation curves between the 3D corrugated structure and the homogenized plate for tensile following MD, CD, and 45°. The maximum difference between the two models is less than 2%. The homogenized model describes the tensile test very satisfactorily.

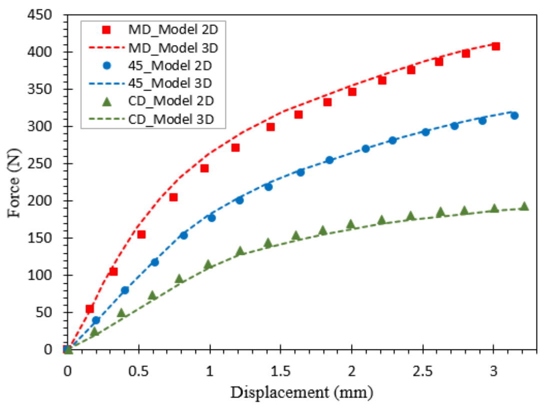

Fig. 8. Comparison of the force vs elongation curves between the 3D corrugated structure and the homogenized plate.

The comparison of the CPU times of the simulations between the 3D corrugated structure and the homogenized plate models is given in Table 3. We find that our homogenization model makes it possible to reduce the CPU time by a factor of 3 up to 6 times.

Direction	Times CPU (s)		Errors
	Model 3D	Model 2D	
MD	361	109	3.3 times
45^0	754	293	2.57 times
CD	511	91	5.6 times

Table 3. CPU time (s) Comparison.

3.2. Validation of the equivalence model by three-point bending test

In the study of Wang et al. (2018), a three-point bending test was performed for corrugated boards. The result is that the relationship between stress and strain is calculated through formulas (18) and (19). Where σ and ε are the stress and strain in the middle of the specimen on the outer fiber of the tensile part, respectively. Therefore, to extend the tensile behavior of the proposed homogenization model, we present a numerical simulation for the 3-point bending test of corrugated board (type B) with sample size, and material parameters. The data and boundary conditions are the same as in the study of Wang et al.

$$\sigma = \frac{3PL}{2bd^2} \tag{21}$$

$$\varepsilon = \frac{6Dd}{L^2} \tag{22}$$

where σ, and ε are the stress and strain in the middle of the specimen on the outer fiber, P is the applied load, D is the deflection in the center of the specimen, L, b, and d are the distance between the fixed supports, width and thickness of the test specimen.

Compare the numerical simulation results with the experimental results shown in Fig. 9 and Fig. 10. Figure 9 shows the similarity of the results of deformation under bending between the two models. Figure 10 shows the relationship curve between bending strain and bending stress of the experiment, 3D model, and 2D homogenous model of corrugated board. The results show that the difference between the three curves is very small. On the other hand, the calculation time for the 3D model is 3541s, while the simulation time for the 2D homogenizer model is very fast, using only 181s (*almost 19.57 times faster*).

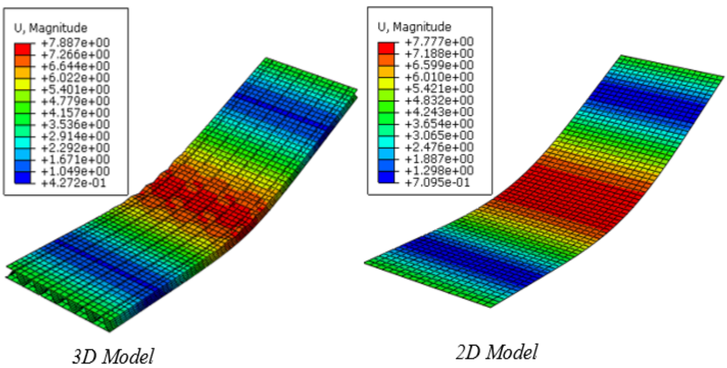

Fig. 9. Comparison of bending strain between 3D model and 2D homogenous model.

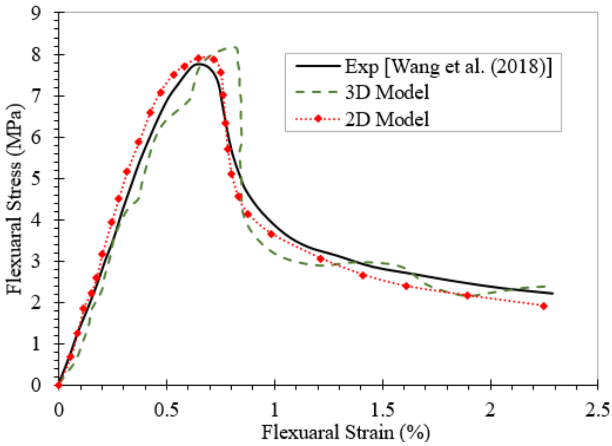

Fig. 10. Comparison of bending stress-strain.

4. Conclusions

In this study, a 2D finite element model describing the plastic properties of corrugated core cardboard is built by using the homogenization method. This model replaces the full 3D model for studying the plastic behavior of corrugated cardboard. Comparing the results between the two models, the 3D composite structure and the 2D homogenous plate, and with experimental results, show very good consistency. The proposed model allows to save computation time and reduces the preparation of geometries. Especially when calculating for large-sized sandwich panels.

Acknowledgments: This research is supported by Hung Vuong University under grant number 19/2022/HĐKH-HV19.2022

References

B.T. Cao, B. Hou, Y.L. Li, H. Zhao (2017). An experimental study on the impact behavior of multilayer sandwich with corrugated cores, International Journal of Solids and Structures, 109, 33–45.

Cenk Kılıçaslan, Mustafa Güden, İsmet Kutlay Odac, Alper Taşdemirci (2014). Experimental and numerical studies on the quasi-static and dynamic crushing responses of multi-layer trapezoidal aluminum corrugated sandwiches, Thin-Walled Structures 78 (2014) 70–78

Damian Mrówczyński and Tomasz Garbowski (2023), Influence of Imperfections on the Effective Stiffness of Multilayer Corrugated Board, Materials 2023, 16, 1295.

Damian Mrówczyński, Anna Knitter-Piątkowska, and Tomasz Garbowski (2022), Numerical Homogenization of Single-Walled Corrugated Board with Imperfections, Appl. Sci. 2022, 12, 9632.

Luong, V.D., Bonnin, A.-S., Abbès, F., Nolot, J.B., Erre, D. and Abbès, A (2020). Finite element and experimental investigation on the effect of repetitive shock in corrugated cardboard packaging, J. Appl. Comput. Mech., vol7.

N. Talbi, A. Batti, R. Ayad, Y.Q. Guo (2009). An analytical homogenization model for finite element modeling of corrugated cardboard, Composite Structures, 88, p. 280–289.

Marc R. Schultz, Leonard Oremont (2011). Compression Behavior of Fluted-Core Composite Panels. In Conference: 52nd AIAA/ASME/ASCE/AHS/ASC Structures, Structural Dynamics and Materials, pp 1-16.

Mäkelä P, (2003). Östlund S.Orthotropic elastic-plastic material model for paper materials, Int J Solids Struct, 40, p. 5599–5620.

M.R.M. Rejab, W.J. Cantwell (2013), The mechanical behavior of corrugated-core sandwich panels, Composites: Part B 47 (2013) 267–277.

PTM Duong, B Abbes, YM Li, AD Hammou, M Makhlouf, and YQ Guo (2012). An analytic homogenization model for shear–torsion coupling problems of double corrugated core sandwich plates, Journal of Composite Materials, 47(11) 1327–1341.

Jongmin Park, Sewon Chang, and Hyun Mo Jung (2020), Numerical Prediction of Equivalent Mechanical Properties of Corrugated Paperboard by 3D Finite Element Analysis, Appl. Sci., 10, 7973.

Kyung-Jo Park, Kang Jung, Young-Wann Kim (2016), Evaluation of homogenized effective properties for corrugated composite panels, Composite Structures 140, p. 644–654

T.J. Lu, L. Valdevit, A.G. Evans (2005). Active cooling by metallic sandwich structures with periodic cores, Progress in Materials Science 50, 789–815.

Rajesh Kumar Boorle. Bending, (2014). Vibration and Vibro-Acoustic Analysis of Composite Sandwich Plates with Corrugated Core, Ph.D. Thesis, University of Michigan-Dearborn.

V. Dung Luong, Fazilay Abbès, Boussad Abbès, P. T. Minh Duong, Jean-Baptiste Nolot, Damien Erre and Ying-Qiao Guo (2018). Finite Element Simulation of the Strength of Corrugated Board Boxes Under Impact Dynamics, In book: Proceedings of the International Conference on Advances in Computational Mechanics.

Wan-Shu Chang and T. Krauthammer (2006), Elasto-Plastic Analysis of Corrugated-Core Sandwich Plates, Mechanics of Advanced Materials and Structures, 13:151–160

Xiaoxia Huang, Chen Zhou, Zhijin Wang (2020), Homogenization of V-pattern Folded Core Sandwich Panels Using Finite Element Simulation, 11th International Conference on Mechanical and Aerospace Engineering.

Z. W. Wang and Y. C. Sun (2018). Experimental investigation on bending fatigue failure of corrugated paperboard. Packag. Technol. Sci., vol. 31, no 9, pp. 601–609.

Z. ABOURA, N. TALBI, S. ALLAOUI & M.L BENZEGGAGH (2004), Elastic behavior of corrugated cardboard: Experiments and Modeling, Composite Structures, Volume 63, Issue 1, Pages 53-62.